Available online at www.CivileJournal.org

Civil Engineering Journal

(E-ISSN: 2476-3055; ISSN: 2676-6957)

Vol. 10, No. 03, March, 2024

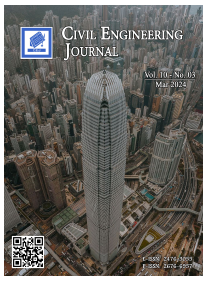

Application of the Arrhenius Equation in Predicting the Temperature Susceptibility of Unmodified and Modified Bituminous Binder

Tangudu Srikanth [1], Ajithkumar Padmarekha [1*]

[1] *Department of Civil Engineering, SRM Institute of Science and Technology, Kattankulathur– 603203, Tamil Nadu, India.*

Received 10 October 2023; Revised 09 February 2024; Accepted 15 February 2024; Published 01 March 2024

Abstract

Bitumen is a temperature-susceptible material. The performance of the bitumen largely depends on the sensitivity of its characteristic properties to the variation in temperature. This paper uses the Arrhenius equation to predict the temperature-sensitive properties of various bitumens. Three modified and unmodified binders of various grades were tested under study shear, frequency mode (oscillatory shearing), and time mode (multiple stress creep and recovery) at different temperatures from 10 to 70ºC. This paper focuses on the activation energy to understand the temperature-susceptible behavior of the bitumen and the influence of aging on the bitumen. To analyze the temperature susceptibility of the bitumen, Steady shear, MSCR, and LAOS tests were performed. From these tests, parameters such as viscosity, dynamic modulus, energy dissipation, and creep compliance at different temperatures were observed to follow the Arrhenius equation. The activation energy constant of the Arrhenius equation is found to vary with the characteristic function used. It is also statistically proven that the activation energy depends on the shear rate or shear stress, indicating that the temperature-susceptible properties of the bitumen are shear rate-dependent. Also, as the bitumen ages, its temperature-susceptible properties improve.

Keywords: Activation Energy; Aging of Bitumen; Arrhenius Equation; Creep Compliance; Energy Dissipation; F Test; Temperature Susceptibility.

1. Introduction

Bitumen is extensively used as a binder in the paving of roads. Bitumen is a viscoelastic material, and its characteristic properties largely depend on temperature. The temperature of bitumen in the pavement may vary from -10 °C to 70°C [1]. This range of temperature depends on the geographical location. At higher temperatures, bitumen exhibits viscoelastic fluid-like behavior and as the temperature reduces, the behavior changes to viscoelastic solid-like and further to elastic [2, 3]. The performance of bitumen largely depends on its temperature-sensitive nature. For instance, if one considers pavement deformation in the pavement, bitumen plays a key role in controlling the deformation. One may demand 'high' viscosity bitumen to control pavement deformation. It is understood that the viscosity of the bitumen depends on the temperature and hence the accumulation of permanent deformation depends on the sensitivity of the viscosity variation with the temperature. The material that exhibits the least variation in its characteristic properties over a range of temperatures is said to be more temperature-susceptible. The temperature-susceptible nature of the binder plays a key role in the selection of the binder. However, the existing methods of grading (viscosity grade and performance grade) do not consider the temperature-susceptible properties of bitumen [4, 5].

* Corresponding author: padmarea@srmist.edu.in

http://dx.doi.org/10.28991/CEJ-2024-010-03-015

Heukelom [6] made a first attempt to understand the temperature susceptibility of bitumen. The temperature susceptibility chart for bitumen was plotted using penetration, softening temperature, Flash point, and viscosity. The temperature-sensitive characteristics of the bitumen can be understood better using shear viscosity and oscillatory shear tests [2, 7]. Padmarekha and Krishnan [2] captured the viscoelastic solid-fluid transition in the temperature range of 20 to 70 ^{0} C using linear viscoelastic parameters. Nivitha et al. [8] studied the temperature sensitivity of the bitumen using Fourier transform infrared (FTIR) spectroscopy and observed viscoelastic solid-fluid transformation in the temperature range of 35 to 65 ^{0}C. The time-temperature superposition principle (TTSP) has been widely applied to predict the response of bitumen at any temperature if the response of the bitumen at a reference temperature is known. For this purpose, it is assumed that the temperature sensitivity characteristics of the bitumen follow the William-Landel-Ferry equation (WLF) [9] or the Arrhenius equation [10].

WLF equation was introduced for the polymers, and it is derived based on the free volume theory. A shift factor is introduced to shift the characteristic properties measured at any temperature to the reference temperature. The shift factor (a_T) is given in Equation 1.

$$\log a_T = \frac{-C_1(T - T_{ref})}{C_2 + (T - T_{ref})}, \quad (1)$$

where, T_{ref} is the reference temperature, C_1 and C_2 are constants. Williams et al. [9], proposed C_1 as 8.86 and C_2 as 101.6 K and these constants are considered universal constants. WLF equation is applicable above the glass transition temperature. Literature on bitumen proposed different combinations of WLF constants for bitumen [11, 12]. There is a complexity in applying the WLF equation is the transitory regime of bitumen [13].

Arrhenius's equation describes the effect of temperature on the viscosity of the material and it is given in Equation 2.

$$\ln \lambda = \ln K + \left[\frac{E}{RT}\right], \quad (2)$$

where λ is the relaxation time, T is the temperature, E is an activation energy constant, K and R are other constants. Cheung & Cebon [14] proposed that the temperature sensitivity of the bitumen below its glass transition temperature follows the Arrhenius relationship, and at higher temperatures, the WLF relationship was found to be valid. Atul Narayan et al. [15] quantified the temperature-susceptible property of modified and unmodified bitumen at the high-temperature region using the Arrhenius equation and suggested a methodology for high-temperature bitumen grading activation energy constant. In the current investigation activation energy is used to understand the temperature-susceptible properties of the bitumen.

Viscoelastic characteristic parameters such as viscosity, dynamic modulus, and creep compliances were used to determine the activation energy of the binder. Maze [16] applied this activation energy concept to the EVA-modified binder, and the typical activation energy was observed to be 67 kJ/mol. Salomon & Zhai [17] observed the activation energy of the bitumen to vary from 44 kJ/mol to 90 kJ/mol for neat and modified binders. These activation energy values were obtained from the viscosity of the binders measured at 110 and 160 ºC. It was also observed that the same grade (PG) of binders exhibited significantly different activation energy. Dongre et al. [18] reported activation energy between 192 to 243 kJ/mol for six different bitumen's. Salomon & Zhai [19] used the activation energy obtained from the viscosity measured between 80 and 200 °C to rank the temperature susceptibility of different asphalt binders. Saboo et al. [20] reported the activation energy values calculated from the creep compliance, and a new ranking parameter was defined.

The activation energy of bitumen was found to vary with factors such as binder type, aging condition, modifier type, and viscoelastic characteristic parameters used. Literature shows inconsistencies in the trend in the variation of activation energy with the above-mentioned parameters. For instance, Garcia-Morales et al. [21] found that polymer addition leads to a reduction in activation energy, while Ait-Kadi et al. [22] found that the presence of polymer in asphalt results in an activation energy increase. Wang et al. [23] observed that chemical-based additives had insignificant effects on the activation energies while wax-based additives significantly decreased the activation energies. Various hypotheses based on the trend in the variation of activation energy have also been proposed. For Instance, Jamshidi et al. [24] related the trend in variation of activation energy with the phase angle and it was observed that the binder with a higher phase angle has higher activation energy. The activation energy was observed to increase on aging [25, 26]. Haider et al. [27] correlated activation energy and performance grading parameters and showed that high viscous binders have higher activation energy. Notani et al. [28] observed that the increase in the percentage of crumb rubber increases the activation energy. Wang et al. [23] established the relation between molecular weight and activation energy. The activation energy decreases as the molecular weight increases.

In addition to the temperature-susceptible characteristic behavior, the response of the bitumen is also shear-susceptible. Raouf and Williams [29], have studied the shear rate susceptibilities of bio-oils, it was observed that the

relationship between the viscosity of bio-oils and temperature and shear rates are log-linear–like bitumen binders. Ingram et al. [30], stated that reduction in the viscosity due to temperature is more significant as compared with shear rate. One can expect that the temperature behavior of the bitumen may depend on its shear susceptibility.

One can see many complexities related to the activation energy, and irrespective of the extent of complexity evolved, AE can be viewed as a tool to predict the temperature-susceptible behavior of bitumen. For this purpose, one needs a clear understanding of how the activation energy of bitumen differs with test protocol, binder type, and aging of bitumen. The steady shear test (for determining mixing and compaction temperature), oscillatory shear test (for performing grading and fatigue damage-related studies), and multiple stress creep and recovery (rutting-related studies) are the widely used test protocols in bitumen characterization. In this experimental investigation, various grades of unmodified bitumen and modified bitumen with different additives (crumb rubber, elastomer, and plastomer) were subjected to steady shear, oscillatory shear, and multiple stress creep and recovery, and the viscosity, dynamic modulus, energy dissipation, and creep compliance were measured at different temperatures. The application of the Arrhenius equation to these parameters was studied and AE's were determined. The significance of the variation in the AE among these characteristic functions was statistically verified. This paper focuses on the activation energy as a tool to understand the temperature susceptible behavior of the bitumen. To understand the influence of aging, the AE was determined for three different aging conditions includes unaged, short-term aged, and long-term aged bitumen. The details of the material used, and the experimental protocol are given in the following section.

2. Research Methodology

Figure 1 shows the flowchart of the research methodology through which the objectives of this study were achieved.

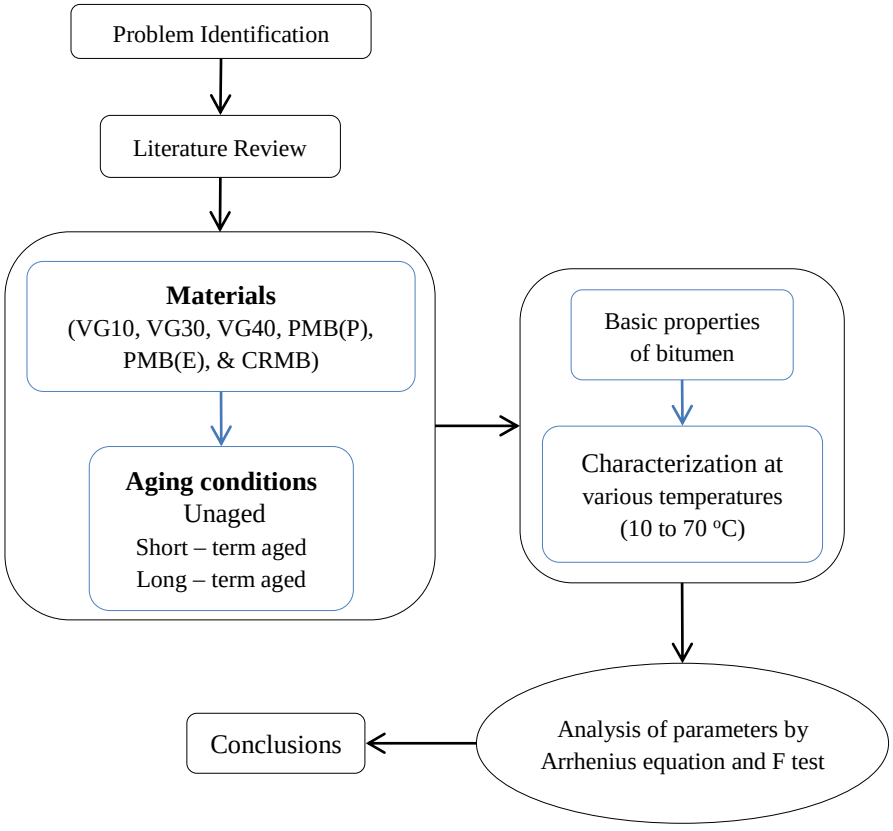

Figure 1. Research methodology flowchart

3. Experimental Investigation

3.1. Materials

This experimental investigation is conducted using six types of bitumen out of which three are unmodified bitumen and others are modified bitumen. The unmodified bitumen of grade VG10, VG30 and VG40 as per IS73, 2018 [4] is used in this experimental investigation. Table 1 lists the basic properties of the unmodified bitumen. From the three modified bitumen used, one is the plastomer-modified bitumen (PMB(P)), the second is elastomer-modified bitumen (PMB(E)), and the third one is the crumb-rubber-modified bitumen(CRMB). The basic properties of modified binders

used in this investigation are given in Table 2. All six binders were tested at unaged (UA), short-term aged (STA) and long-term aged (LTA) conditions. The short-term aging is carried out using a rolling thin film oven following ASTM D2872, 2022 [31]. The short-term aged sample is then subjected to long-term aging in pressure aging vessel following ASTM D6521, 2022 [32].

Table 1. Basic properties of unmodified bitumen

Characteristic properties	VG10	VG30	VG40
Penetration at 25˚C, 0.1 mm, 100 g, 5 s, 0.1 mm	99	61	40
Softening Point, (R&B), ºC	42	48	53
Absolute viscosity at 60˚C, Poises	1143	2677	3640
Kinematic viscosity at 135˚C, cSt	365	510	652
Tests on residue from rolling thin film oven test:			
a) Viscosity ratio at 60˚C	2.29	2.54	3.8
b) Ductility at 25˚C, cm	>100	>100	28
Temperature corresponding to the |G*|/sin δ of 2.1 kPa of short-term aged binder (25 mm plate, 1 mm gap at 10 rad/s), in °C	66.3	71.4	76.1
Temperature corresponding to |G*|sin δ of 5000 kPa of long-term aged binder (8 mm plate, 2 mm gap at 10 rad/s), in °C	15.2	22.9	19.7

Table 2. Basic properties of modified bitumen

Characteristic properties	PMB(P)	PMB(E)	CRMB60
Penetration at 25˚C, 0.1 mm, 100 g, 5 s, 0.1 mm	31	34	25
Softening Point, (R&B), ºC	76	57	66
The elastic recovery of half thread in ductilometer at 15°C, percent	25	64	69
Separation, the difference in softening point (R&B), °C	3.4	3	11
Viscosity at 150°C, Poise	2.6	5	-
Temperature corresponding to the |G*|/sin δ of 2.1 kPa of short-term aged binder (25 mm plate, 1 mm gap at 10 rad/s), in °C	77.9	84.0	93.7
Temperature corresponding to |G*|sin δ of 5000 kPa of long-term aged binder (8 mm plate, 2 mm gap at 10 rad/s), in °C	25.0	17.0	14.7

4. Experimental Methods

Three different sets of experiments were conducted using a dynamic shear rheometer (DSR) of the MCR102 model (Anton Paar make). The first set of experimental investigations is a steady shear test, the second is the large amplitude oscillatory shear testing (LAOS) and the third one is the multiple stress creep and recovery (MSCR) test. All these tests were conducted using parallel plate geometry of 25 mm diameter with a sample height of 2 mm. In the steady shear test, all the materials were sheared at a constant shear rate of 0.5 s^{-1} as shown in Figure 2-a. The temperature of the sample during the test was maintained constant and the material was sheared for 10 minutes. The test was conducted for every 10^0 C temperature increment in the range of 40 to 80^0 C.

In the second set of experimental investigations, the bitumen was subjected to repeated oscillatory shearing in strain-controlled mode using LAOS protocol and the material was continuously sheared for 10 minutes. The strain amplitude, frequency and temperature during shearing were maintained constant during testing as shown in Figure 2-b. The test was conducted for three different strain amplitudes of 1, 5 and 10% and three different frequencies of 1, 5 and 10 Hz. The test was conducted for every 5^0 C temperature increment up to 70^0 C. The lowest temperature for testing each sample is fixed based on the maximum torque of 200 mNm. Also, sufficient care was taken while testing the material at a lower temperature with a 25 mm diameter plate. Table 3 shows the details of LAOS tests conducted for the VG30 grade of bitumen. A total of 224 numbers of LAOS tests were conducted using VG30 bitumen grade. Likewise, the total number of LAOS test conducted on VG10, VG40, PMB(E), PMB(P) and CRMB bitumen were 252, 211, 217, 220 and 217 respectively. During testing, the complete torque and stress waveform data were collected for every 10 cycles of shearing and each waveform data consisted of 512 data points.

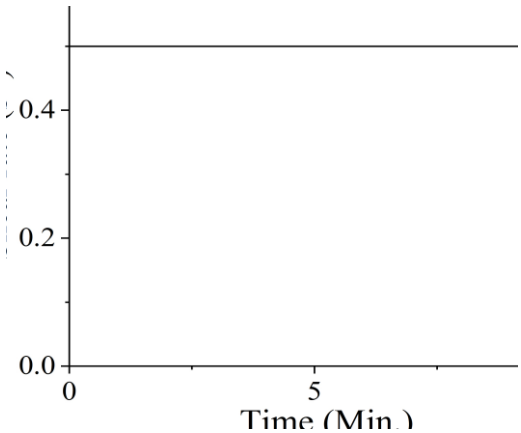

(a) Steady shear test protocol

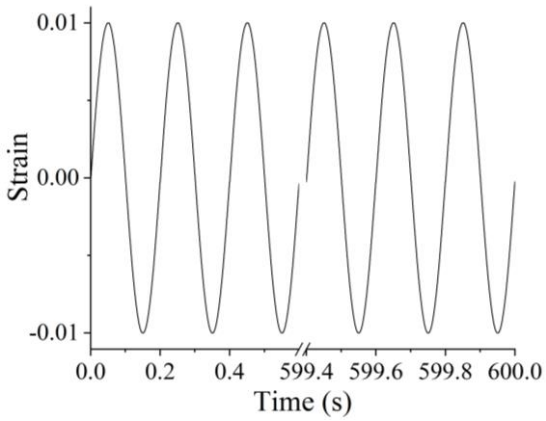

(b) LAOS test protocol – 1% strain and 5 Hz frequency

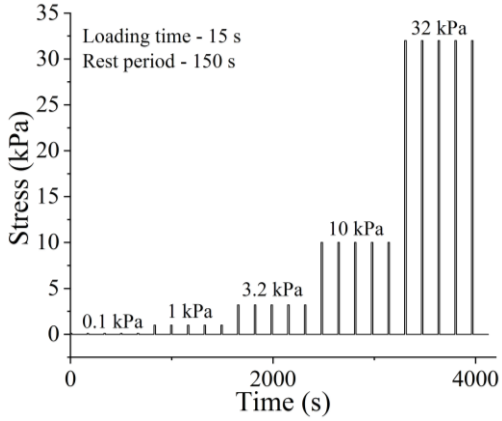

(c) MSCR test protocol

Figure 2. Experimental test protocols

Table 3. LAOS test details of VG30 bitumen

Material aging condition	LAOS			
	Temperature interval (°C)	Strain (%)	Frequency (Hz)	Number of tests
UA	20 – 70	1	1	11
	25 – 70	5		10
	30 – 70	10		9
	25 – 70	1	5	10
	35 – 70	5		8
	35 – 70	10		8
	25 – 70	1	10	10
	35 – 70	5		8
	40 – 70	10		7
STA	20 – 70	1	1	11
	30 – 70	5		9
	30 – 70	10		9
	25 – 70	1	5	10
	35 – 70	5		8
	40 – 70	10		7
	30 – 70	1	10	9
	40 – 70	5		7
	45 – 70	10		6
LTA	25 – 70	1	1	10
	35 – 70	5		8
	35 – 70	10		8
	30 – 70	1	5	9
	40 – 70	5		7
	45 – 70	10		6
	35 – 70	1	10	8
	45 – 70	5		6
	50 – 70	10		5
Total				**224**

The third set of experimental investigations is the repeated creep and recovery test with each cycle of shearing consisting of the application of constant shear stress for 15 seconds followed by a recovery time of 150 seconds. The test was conducted for five different stress magnitudes of 0.1, 1, 3.2, 10 and 32 kPa. Five cycles of loading and unloading were applied at each stress level and the schematic of the MSCR test is shown in Figure 2-c. The temperature during testing was maintained constant and the experiment was conducted for every 5^0 C increment in the temperature range of 20 to 70^0 C.Figure 3 shows the images of the equipment, sample preparations, sample testing.

(a) Equipment

(b)Sample Preparation

(c)Placing of sample in the equipment

(d)Testing of sample

Figure 3. Images of the equipment, sample preparations, sample testing

5. Results and Discussion

5.1. Steady Shear Test

Figure 4 shows the apparent viscosity of selected samples (VG30-UA and PMB(P)-UA) measured at different temperatures. As expected, the apparent viscosity reduced with an increase in temperature. The viscosity reached a steady state after a few seconds of shearing and a steady viscosity value at 200^{th} seconds was selected for further analysis. Figure 5 compares the viscosity of different binders at different aging conditions. At any given temperature, the addition of a modifier increased the viscosity of the binder. As expected, the viscosity increased with aging and the percentage increase with aging varied with binder and temperature of interest. PMB(E) binder at 30°C exhibited a maximum percentage increase of 92% from UA to LTA condition and CRMB binder at 80°C exhibited a minimum percentage increase of 53%.

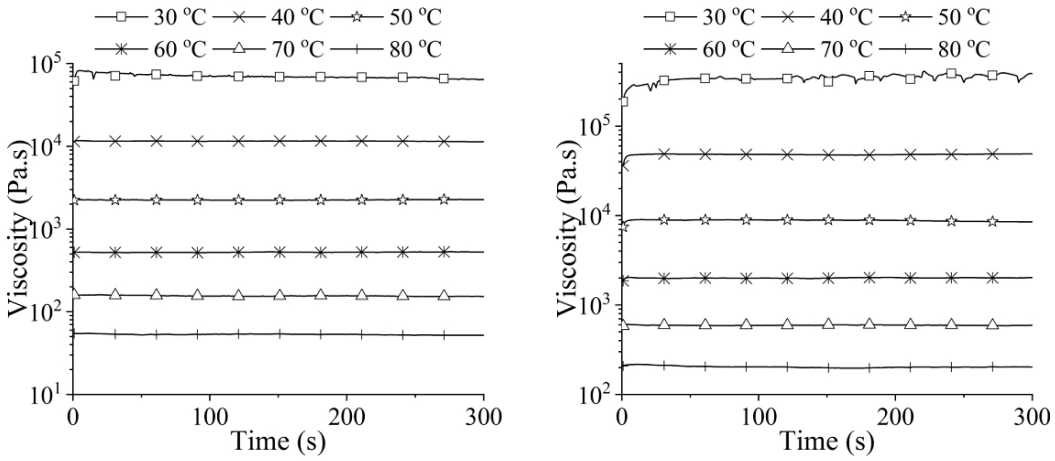

(a) VG30-UA (b) PMB(E)-UA

Figure 4. Steady shear viscosity at different temperatures

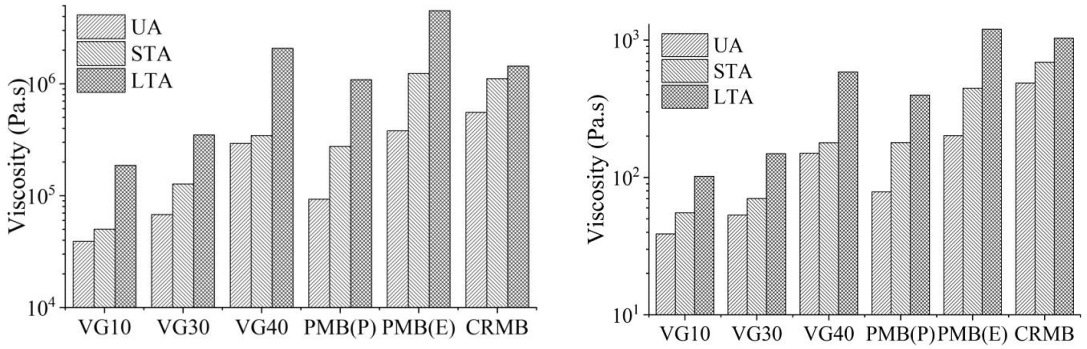

(a) 30^0C (b) 80^0C

Figure 5. Comparison of viscosity of different binders at different aging conditions

Among six binders tested, the viscosity of CRMB binder is found to be less prone to aging change. The variation of viscosity with temperature of all binders tested and for all aging conditions is shown in Figure 6. The logarithm of viscosity exhibited a linear relation with the inverse of temperature measured in K^{-1}. The Arrhenius equation (discussed in equation 1) is fitted to the viscosity-temperature experimental data and the slope of the linear line is considered as the Activation Energy (AE). The AE of all the samples tested are tabulated in Table 4. All the values tabulated here correspond to R^2 of 0.99 or more. The AE constant represents the temperature-susceptible nature of the binder. The material with high value of AE indicates high sensitivity to changes in temperature. AE determined based on viscosity was observed to increase with aging. In the unmodified binder, VG10 is observed to be least susceptible to change in temperature when compared to VG30 and VG40. In a modified binder CRMB is least susceptible to change in temperature. From Table 4 one can state that the AE of all STA binders except VG30 increases to about 2 %, whereas the VG30 STA binder increases to about 7 % when compared with the UA binder. Similarly, the AE of all LTA binders except CRMB increases to about 10 %, whereas CRMB LTA binder increases to about 4 % when compared with the UA binder.

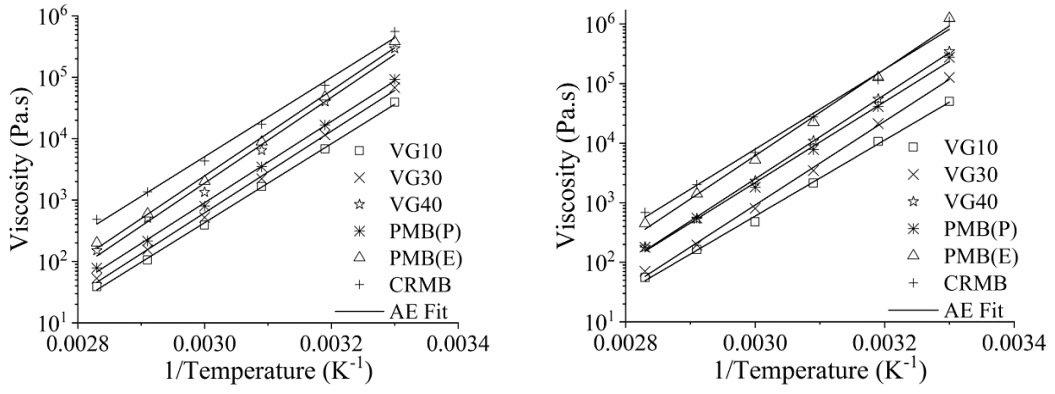

a) Unaged binders b) Short-term aged binders

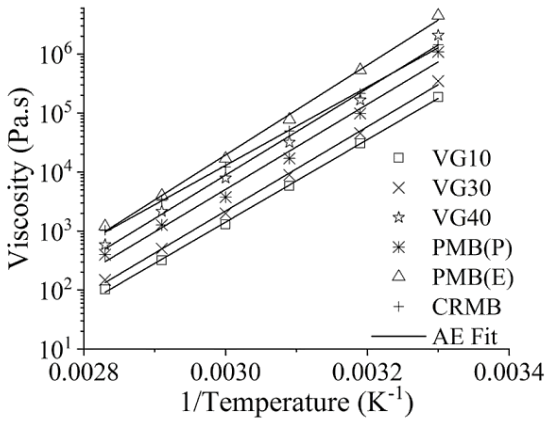

c) Long-term aged binders

Figure 6. Viscosity – temperature relation of various binders and the corresponding AE fit

Table 4. Activation energy for different bitumen based on the viscosity

Binder	Activation Energy (kJ/mol)		
	UA	STA	LTA
VG10	123	122	134
VG30	127	135	137
VG40	134	135	141
PMB(P)	127	130	138
PMB(E)	133	139	146
CRMB	124	129	127

The AE of the binders was compared with Salomon and Zhai [17, 19] and was observed to follow the trend.

5.2. Oscillatory Shear Testing

5.2.1. Activation Energy form Dynamic Modulus

In the experimental investigation, the oscillatory shear test was conducted by selecting the strain amplitude in the linear and nonlinear regime, and the complete stress, strain, and strain rate waveform was recorded using the LAOS protocol. The sample stress, strain, and strain rate waveform data recorded for CRMB-LTA binder at 10% strain amplitude, 10 Hz frequency, and 50°C is shown in Figure 7-a. The dynamic modulus is computed as the ratio of first harmonic stress to strain amplitude. The harmonic stress intensity is computed using the Fast Fourier Transform (FFT) algorithm. The FFT of the sample stress waveform is shown in Figure 7-b. From the FFT results, first-order harmonic is used in the computation of dynamic modulus.

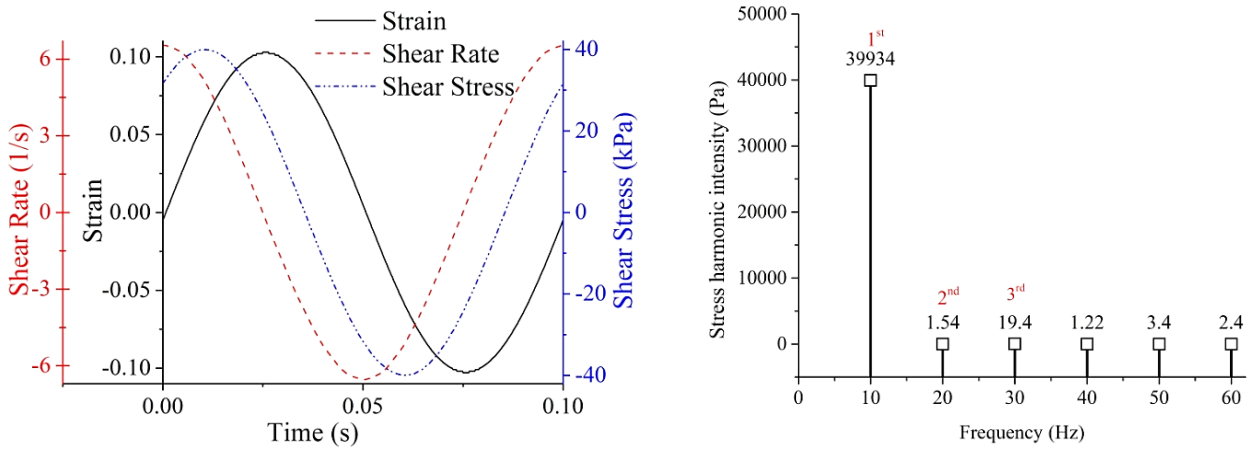

(a) Sample waveform (b) Harmonic intensity of stress waveform

Figure 7. Shear stress waveform and the corresponding harmonic intensity

Figure 8 shows the dynamic modulus of long-term aged CRMB binder when tested at 1 and 10 Hz frequency. The variation in dynamic modulus with the inverse of temperature follows the Arrhenius equation and the slope (AE) is observed to be independent of frequency and the strain amplitude. The dynamic modulus of various binders measured at 5% strain amplitude, 5 Hz frequency at different temperatures and the corresponding AE fit for each binder is shown in Figure 9. The corresponding AE is tabulated in Table 5. The AE based on dynamic modulus decreased on aging unlike AE obtained based on the steady shear viscosity value. From Table 5 one can state that the AE of all STA binders decreased to about 1 % when compared with the UA binder. Similarly, the AE of all LTA binders except CRMB decreased to about 3 %, whereas the CRMB LTA binder decreased to about 9 % when compared with the UA binder.

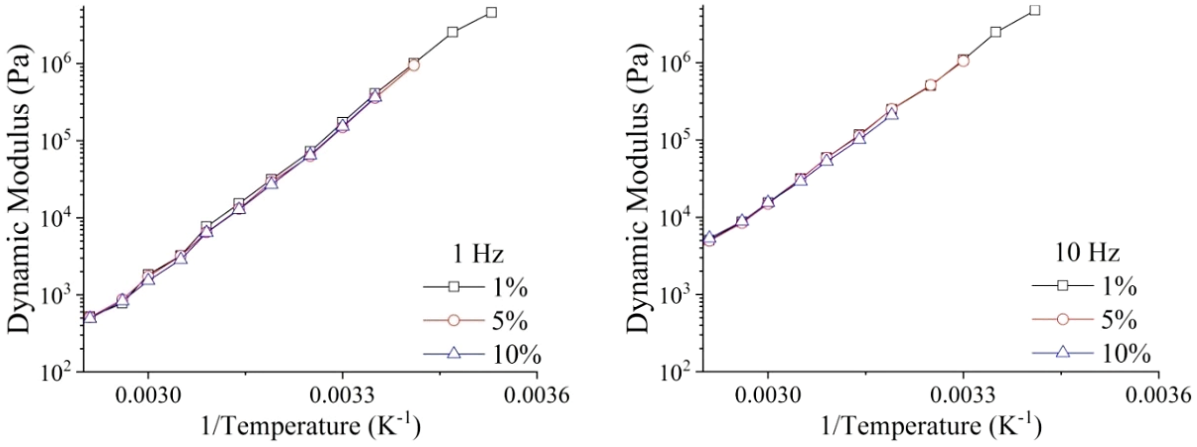

(a) 1 Hz (b) 10 Hz

Figure 8. Variation of dynamic modulus with temperature inverse – CRMB-LTA binder

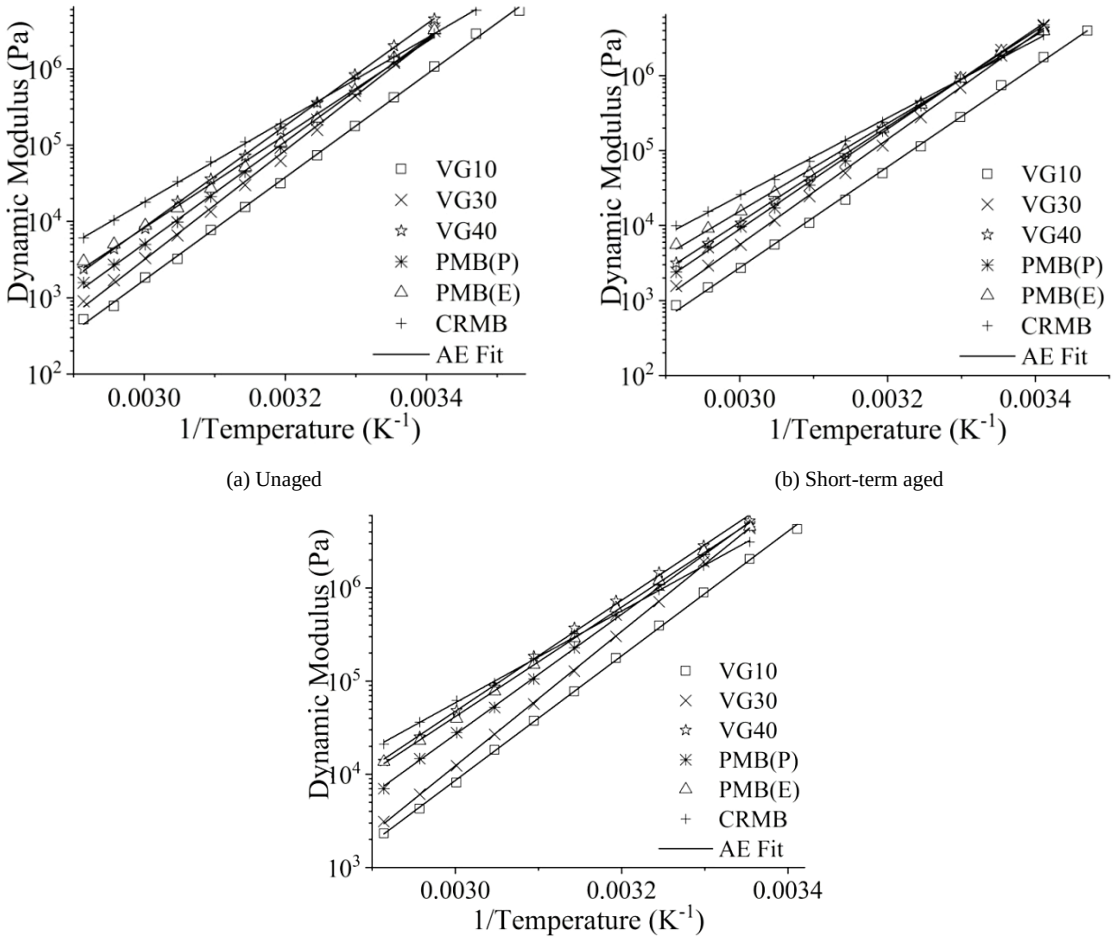

(a) Unaged (b) Short-term aged

(c) Long-term aged

Figure 9. Dynamic modulus – temperature relation of binders and the corresponding AE fit

Table 5. Activation energy for different bitumen based on Dynamic modulus

Binder	Activation Energy (kJ/mol)		
	UA	STA	LTA
VG10	129	129	128
VG30	138	137	134
VG40	127	122	114
PMB(P)	128	128	123
PMB(E)	117	113	113
CRMB	103	99	94

5.2.2. Activation Energy form Energy Dissipation (ED)

The viscoelastic material dissipates energy and the extent of dissipation depends on the temperature of interest. When the material is subjected to sinusoidal strain, the resultant stress waveform may contain higher-order harmonic contribution. It is understood that the energy dissipation due to sinusoidal strain is purely due do the first-order harmonic stress [33]. Hence, the energy dissipation is computed using Equation 3, where ϵ_1 represents first-order harmonic strain, σ_1 is the first-order harmonic stress and δ_1 is the corresponding lag. Here, in the strain-controlled test, the material is subjected to sinusoidal strain and hence ϵ_1 is the same as the strain amplitude.

$$ED = \pi \epsilon_1 \sigma_1 \sin \delta_1. \quad (3)$$

Figure 10 shows the comparison ED of different binders at UA, STA, and LTA conditions. In the strain-controlled test, ED decreases with temperature and it exhibited exponential decrease with temperature. The ED at any given temperature increases with aging. The ED is also expected to be dependent on frequency and strain amplitude. The variation of ED with temperature and shear rate is shown in Figure 11. At any given ED increased with an increase in shear rate. Further, the temperature dependency of ED is captured using the Arrhenius equation. The shear rate dependency of ED is captured from the variation of AE with the shear rate.

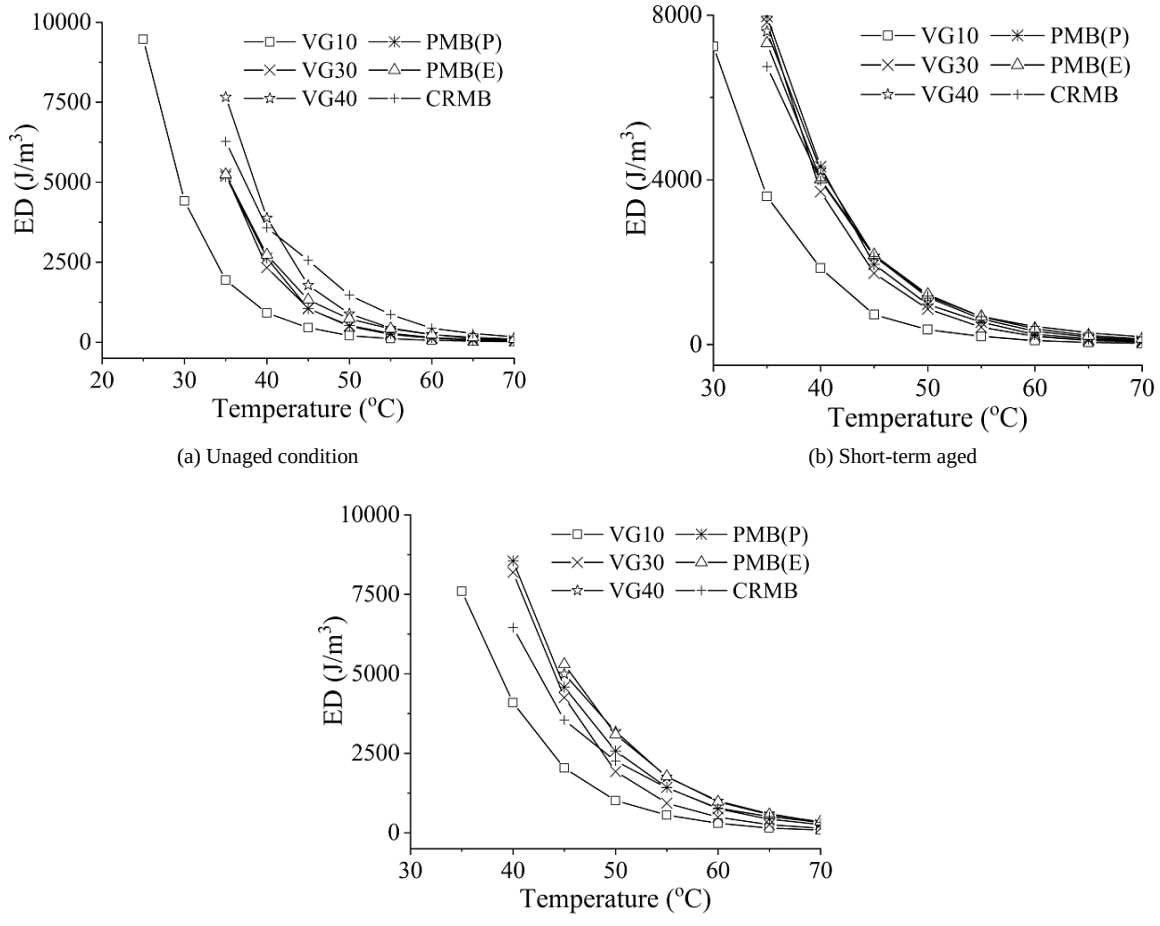

(a) Unaged condition

(b) Short-term aged

(c) Long-term aged

Figure 10. ED of unmodified and modified binders at different aging conditions at 5% strain amplitude and 5 Hz frequency

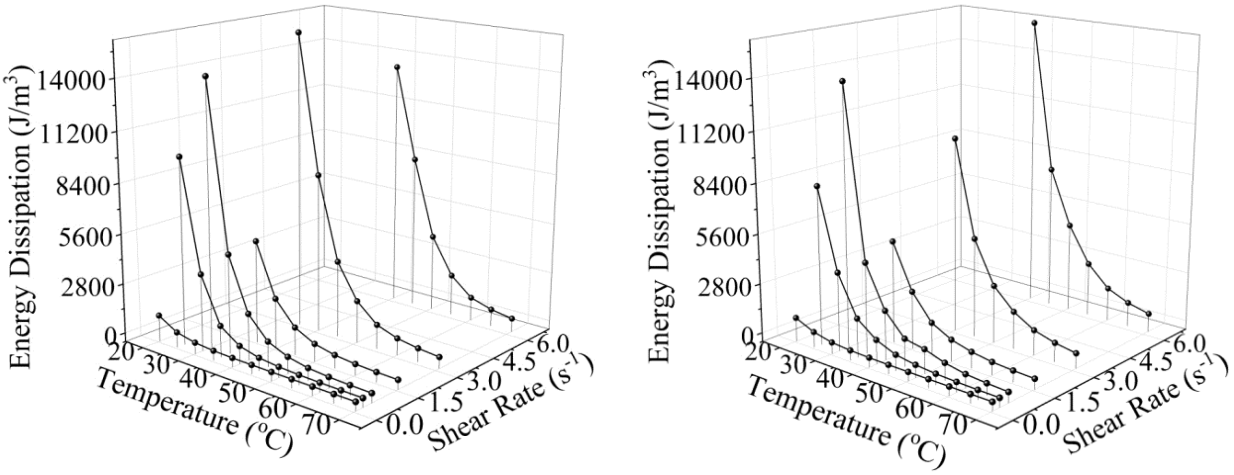

(a) VG30-UA (b) PMB(E)-UA

Figure 11. Variation of ED with shear rate and temperature

Figure 12 shows the logarithm variation of ED of selected samples with the inverse of temperature. The logarithm of ED with the inverse of temperature at all frequencies and strain amplitude tested exhibited a linear relation. The Arrhenius equation is fitted to an ED function and the corresponding slope value (AE) for the R2 of 0.99 for CRMB binder at UA, STA, and LTA condition is tabulated in Table 6. AE decreased with aging. Also, AE is found to depend on the shear rate. From Table 6 one can state that AE is a dependent of shear rate. It was also observed that the AE of all the STA binders decreased to about 2 % at the low shear rate and 18 % at the high shear rate. A similar, trend was observed in the other bonders also.

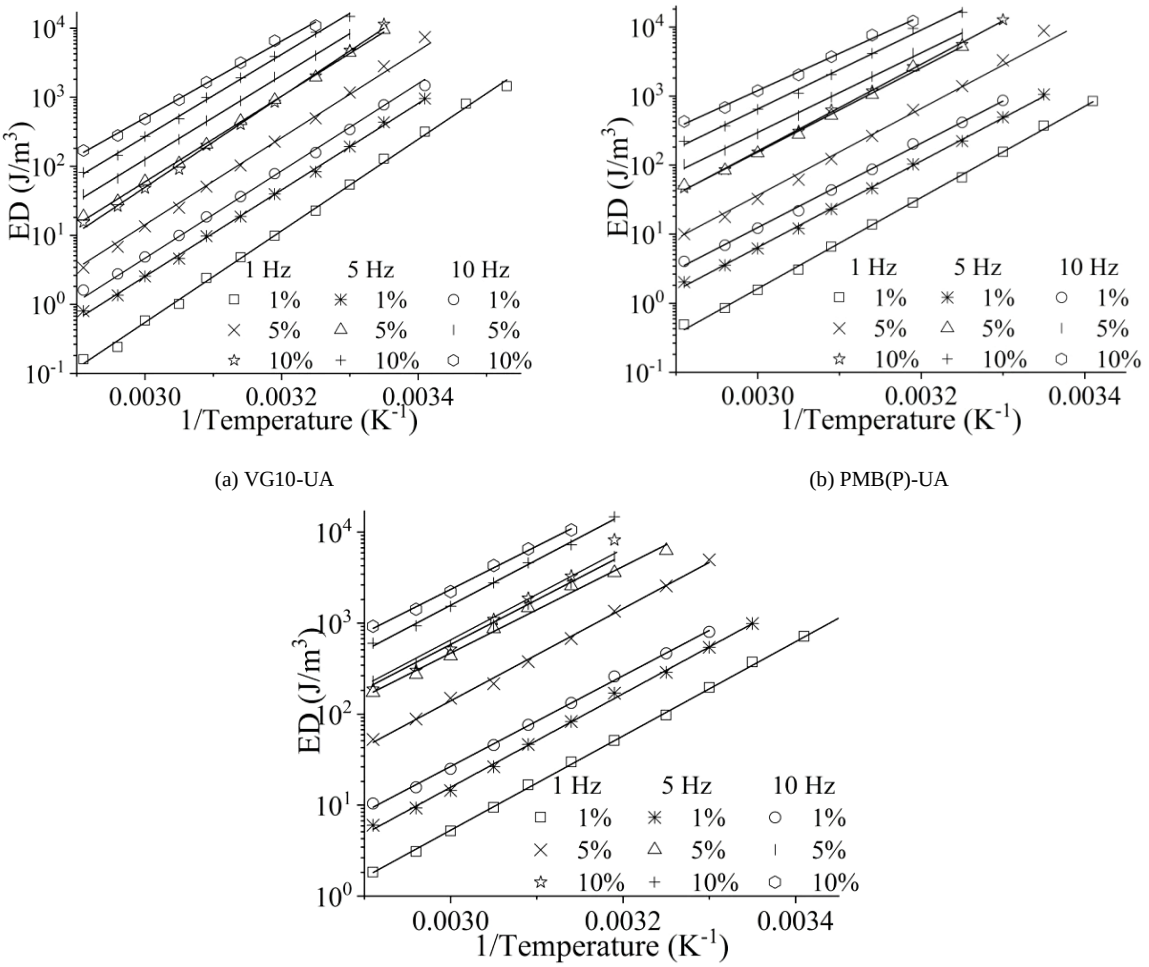

(a) VG10-UA (b) PMB(P)-UA

(c) CRMB-UA

Figure 12. Variation of ED with temperature inverse for different UA binders

Table 6. Activation Energy of CRMB binder computed from Energy dissipation

Frequency (Hz)	Strain (%)	Shear rate (s^{-1})	AE (kJ/mol)		
			UA	RTFO	PAV
1	1	0.0625	99	97	90
	5	0.312	97	92	92
	10	0.623	112	91	81
5	1	0.312	98	92	91
	5	1.57	91	91	90
	10	3.12	95	87	79
10	1	0.623	110	90	81
	5	3.12	94	88	79
	10	6.23	91	85	77

Figure 13 shows the variation of AE with shear rate. With the increase in shear rate, the activation energy constant decreased for all the binders. The shear rate dependency is more prominently observed at the lower shear rate.

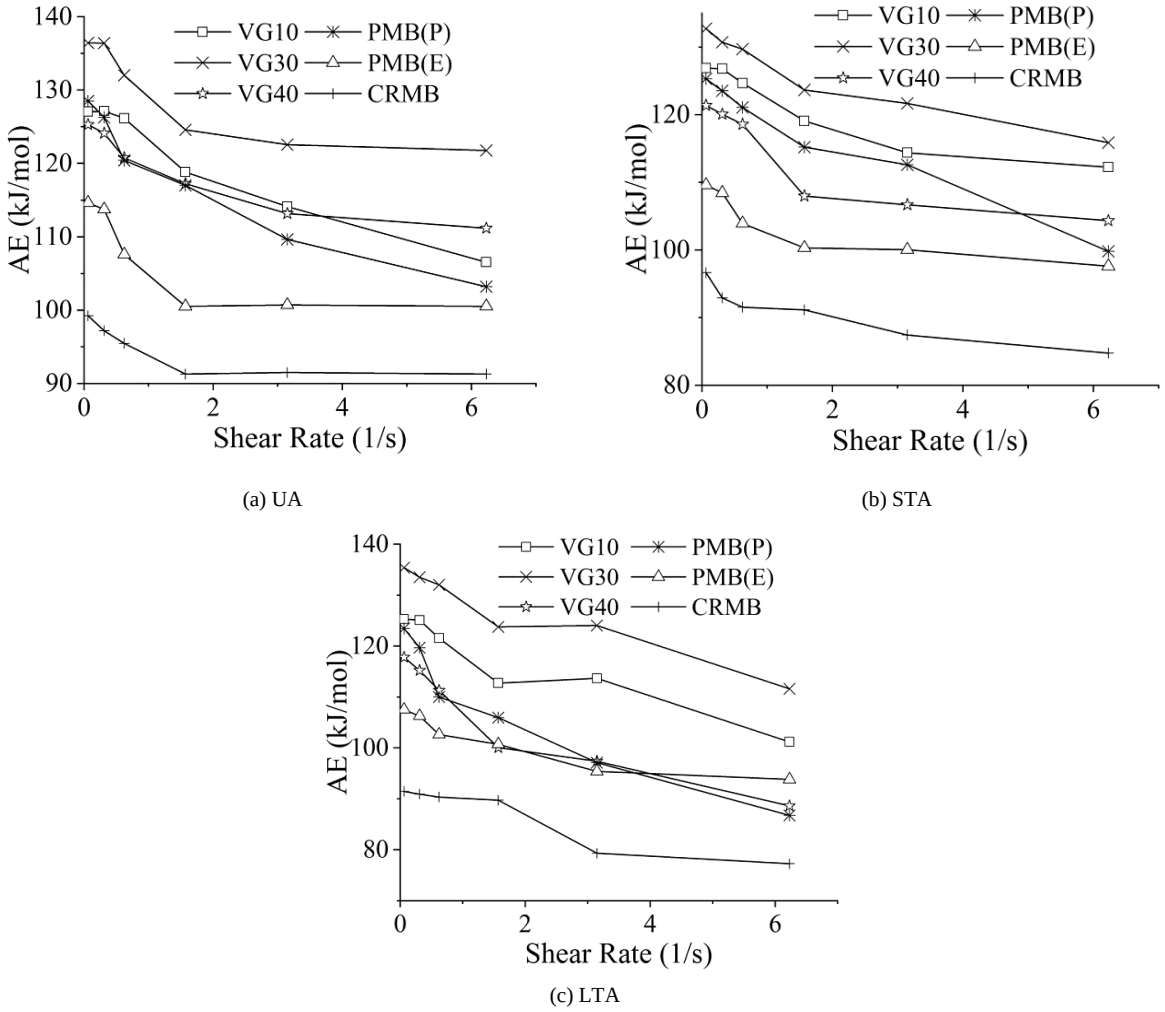

(a) UA

(b) STA

(c) LTA

Figure 13. Variation of AE as a function of shear rate for all binders of different aging conditions

To check whether the influence of shear rate on AE is significant, ANOVA analysis (F test) is carried out. For this purpose, AE is separated into three groups based on the shear rate (SR). AE corresponding to SR ≤ 0.315 are grouped under one, AE corresponding to SR between 0.315 and 1.570 are considered under the second group and AE corresponding to SR greater than 1.570 under the third group. Table 7 shows the grouped data of the VG30-UA binder

for ANOVA analysis. It is hypothesized that the mean activation energy of the binder is the same for each of the three levels of shear rate and the F value was determined using Equation 4.

$$F = \frac{SS_{Tr}/_{Dof}}{SS_E/_{error}} \quad (4)$$

Here, $\frac{SS_{Tr}}{Dof}$ represents the mean sum of squares of AE between the groups and $\frac{SS_E}{error}$ represents the mean sum of squares of AE within the groups. SS_{Tr}andSS_E are computed using Equations 5 to 7.

$$SS_T = \sum_{i=1}^{k}\sum_{j=1}^{n} x_{ij}^2 - \frac{1}{kn}T^2 \quad (5)$$

$$SS_{Tr} = \frac{1}{n}\sum_{i=1}^{k} T_i^2 - \frac{1}{kn}T^2 \quad (6)$$

$$SS_E = SS_T - SS_{Tr} \quad (7)$$

Here, x_{ij} represents activation energy, T represents the group total, k is the number of groups, and, n is the number of observations in a group. Dof represents the degree of freedom which is $n-1$and, $error$ is given by $n(n-1)$.The F value of all the samples were documented in Table 8. The F value corresponding 5% level of significance was found to be 5.143. From Table 8, it is clear that F values of energy dissipation-based AE for most of the binders are shear rate dependent. Hence, the AE obtained from the energy dissipation was found to depend on the strain amplitude and the frequency of shearing. Here, it has to be highlighted that AE obtained from the dynamic modulus is independent of strain amplitude and frequency.

Table 7. Grouping of ED-based AE of VG30-UA binder for ANOVA

Sl. No.	SR - Shear Rate, AE - Activation Energy	Observations			Total (T)	Mean (s)
1	SR ≤ 0.3150	0.0625	0.3120	0.3150	-	-
	AE	136	136	128	401	134
2	0.3150 < SR ≤ 1.5700	0.6230	0.6250	1.5700	-	-
	AE	132	123	125	379	126
3	SR > 1.5700	3.1200	3.1500	6.2300	-	-
	AE	123	119	122	363	121
					1143	127

Table 8. F value for Energy dissipation and Jnr

Binder	UA		STA		LTA	
	ED	J_{nr}	ED	J_{nr}	ED	J_{nr}
VG10	5.2	74.7	5.4	64.4	1.7	70.7
VG30	6.7	39.1	1.9	298.6	1.1	260.5
VG40	5.6	40.8	5.3	208.6	5.2	94.1
PMB(P)	16.5	125.5	1.6	193.1	5.2	96.7
PMB(E)	9.7	39.1	10.2	30.3	5.4	34.1
CRMB	6.4	43.3	8.7	22.5	9.0	31.6

5.3. Multiple Stress Creep and Recovery Test

Figure 14 shows the sample creep and recovery cycle of CRMB-STA at 1 kPa measured at 30°C. The non-recoverable creep compliance (J_{nr}) is computed from ε_0, the strain at the beginning of any creep cycle and ε_r, the strain measured at the end of the recovery cycle. J_{nr} is computed following Equation 8 stated in ASTM D7405 [34].

$$J_{nr} = \frac{\varepsilon_r - \varepsilon_0}{\sigma} \quad (8)$$

where, σ represents the stress magnitude. Here, it has to be highlighted that the test procedure adopted in this paper differs from the standard ASTM D7405 [34] in two ways. The first difference is the magnitude of stress used for testing. To check the influence of stress on the activation energy, the test was conducted at five different shear stresses 0.1, 1, 3.2, 10, and 32 kPa. This test protocol also differs from the standard MSCR test in terms of creep and recovery time used for testing. An extended creep time of 15 seconds and a recovery time of 150 seconds were chosen to give sufficient time for the material to reach a steady state while shearing. Jnr for each cycle is computed and the average of 5 cycles is used in the computation of activation energy.

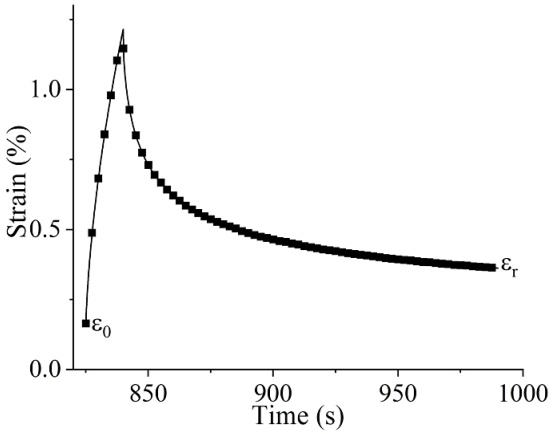

Figure 14. Sample creep and recovery cycle corresponding to CRMB-STA at 1 kPa and 30 ^{0} C

Figure 15 shows the logarithm variation of J_{nr} of selected samples with the inverse of temperature. The logarithm of J_{nr} with the inverse of temperature at all stress levels exhibited a linear relation. The Arrhenius equation is fitted to a J_{nr} function and the corresponding slope value (AE) for the R^2 of 0.99 for PMB(E) binder at UA, STA, and LTA condition is tabulated in Table 9. AE increase on aging. Also, AE is found to depend on the stress. The consolidated AE of the binders was tabulated in Table 10.

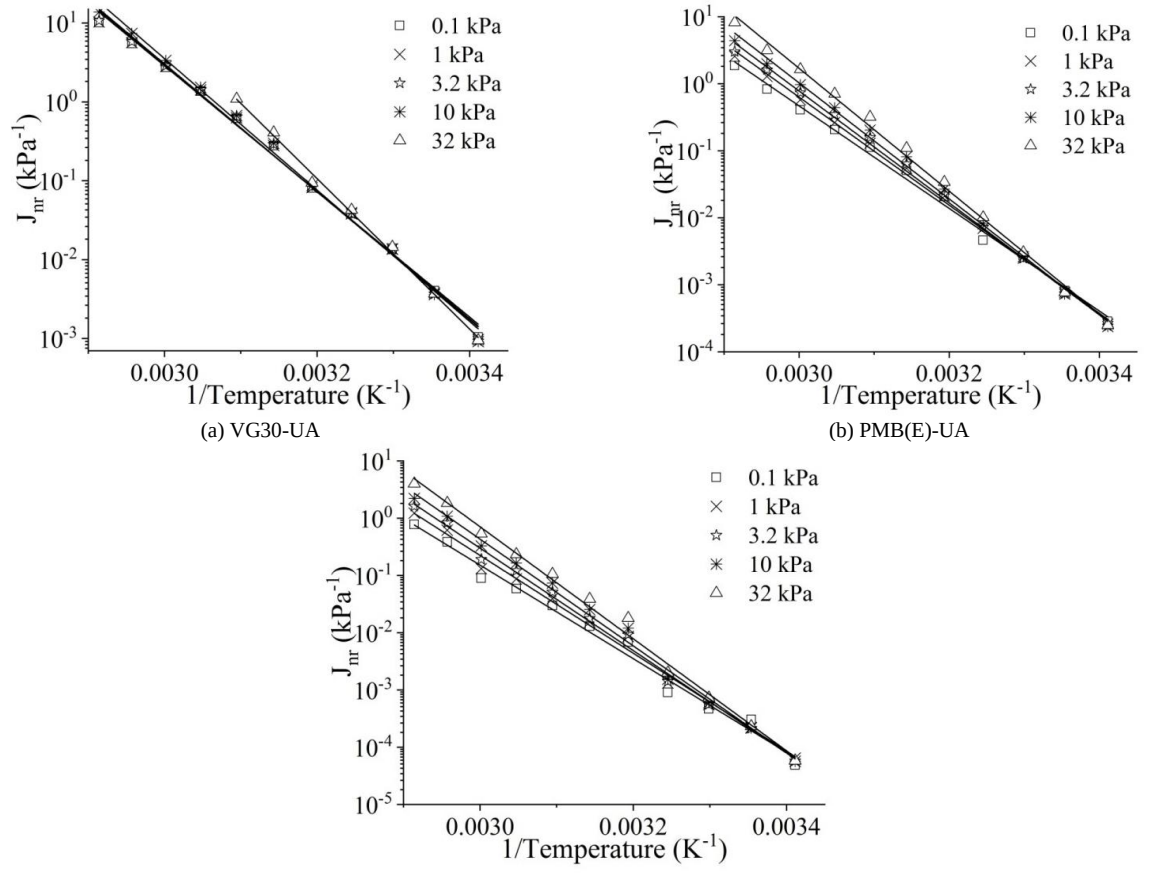

(a) VG30-UA

(b) PMB(E)-UA

(c) CRMB-UA

Figure 15. Variation of creep compliance with temperature inverse for different unaged binders

Table 9. Activation Energy of PMB(E) binder from Jnr

Stress	AE (kJ/mol)		
	UA	RTFO	PAV
0.1 kPa	147	134	150
1 kPa	154	149	158
3.2 kPa	160	158	165
10 kPa	166	166	175
32 kPa	176	179	184

Table 10. Consolidate values of AE from Jnr

Binder	Activation Energy (kJ/mol)		
	UA	STA	LTA
VG10	143 – 194	151 – 188	166 – 179
VG30	152 – 183	156 – 190	165 - 197
VG40	163 – 179	165 -204	171 - 210
PMB(P)	148 – 176	155 – 194	173 - 202
PMB(E)	146 – 176	134 – 179	149 - 184
CRMB	156 – 187	139 – 195	140 - 194

To check the influence of stress in the Jnr-based activation energy, ANOVA analysis is carried out. For this purpose, AE is separated into three groups based on stress levels (σ). AE corresponding to $\sigma \leq 0.1$ kPais considered under Group 1, σ between 0.1 and 10 kPa is considered under Group 2, and $\sigma > 10\ kPa$ is considered under Group 3. The sample grouped data corresponding to VG30-UA is shown in Table 11. The F values for all the samples are determined using Equation 4 and the values are tabulated in Table 8. For the 5% level of significance, the F value in the table indicates that AE depends on the stress level.

Table 11. Grouping of Jnr-based AE of VG30-UA binder for ANOVA

Sl. No.	σ– Stress (kPa), AE - Activation Energy (kJ/mol)	Observations		Total (T)	Mean (s)
1	σ≤ 0.1	0.1	1.0000	-	-
	AE	153	154	307	153
2	0.1 <σ≤ 10	3.2000	10.0000	-	-
	AE	155	160	315	157
3	σ> 10	10.0000	10.0000	-	-
	AE	183	183	365	183
	T - Total and s – mean			**987**	**165**

6. Conclusions

The viscoelastic function of bitumen such as viscosity, dynamic modulus, energy dissipation and non-recoverable creep compliance follows the Arrhenius equation. The activation energy of the Arrhenius equation is viewed as a tool for predicting the temperature susceptibility of bitumen. The following conclusions were made from the detailed experimental investigation:

- The activation energy of any bitumen varied with the choice of viscoelastic parameters.
- The activation energy of bitumen was found to be sensitive to the shear rate/stress variation. This indicates that the temperature susceptibility of the bitumen is shear rate/stress-dependent. The variation is more dominant when the test is conducted at a lower shear rate/stress.
- While comparing the activation energy of PMB(E), and PMB(P) with an unmodified binder, the variation in AE of these binders does not follow any trend. This can be due to differences in shear rate/stress exhibiting low-temperature susceptibility character when compared to unmodified bitumen.

Likewise, the variation in activation energy of bitumen on aging does not follow any trend. For instance, the activation energy based on viscosity and Jnr increases on aging and the activation energy based on dynamic modulus and energy dissipation decreases on aging. This non-trend can be attributed to the difference in the shear-susceptibility of the binder.

7. Declarations

7.1. Author Contributions

Conceptualization, T.S. and A.P.; methodology, T.S. and P.A.; validation, T.S. and P.A.; formal analysis, T.S. and P.A.; investigation, T.S.; resources, T.S. and P.A.; data curation, T.S. and P.A.; writing—original draft preparation, T.S. and P.A.; writing—review and editing, T.S. and P.A.; supervision, P.A.; project administration, P.A. All authors have read and agreed to the published version of the manuscript.

7.2. Data Availability Statement

The data presented in this study are available in the article.

7.3. Funding

The authors would like to acknowledge the Department of Science and Technology, New Delhi, India for financial support (Project no: SERB/F/6157/2018-2019).

7.4. Conflicts of Interest

The authors declare no conflict of interest.

8. References

[1] Nivitha, M. R., & Krishnan, J. M. (2014). Development of Pavement Temperature Contours for India. Journal of The Institution of Engineers (India): Series A, 95(2), 83–90. doi:10.1007/s40030-014-0074-y.

[2] Padmarekha, A., & Krishnan, J. M. (2013). Viscoelastic Transition of Unaged and Aged Asphalt. Journal of Materials in Civil Engineering, 25(12), 1852–1863. doi:10.1061/(asce)mt.1943-5533.0000734.

[3] Nivitha, M. R., & Murali Krishnan, J. (2016). What is Transition Temperature for Bitumen and How to Measure It? Transportation in Developing Economies, 2(1), 1–8. doi:10.1007/s40890-015-0009-y.

[4] IS73. (2013). Paving Bitumen-Specification (4th REVISION). Bureau of Indian Standards, New Delhi, India.

[5] ASTM, D6373-21a. (2023). Standard Specification for Performance-Graded Asphalt Binder. ASTM International, Pennsylvania, United States. doi:10.1520/D6373-21A.

[6] Heukelom, W. (1969). A bitumen test data chart for showing the effect of temperature on the mechanical behavior of asphaltic bitumens. Institute of Petroleum, 55(5460), 404-417.

[7] Storm, D. A., Barresi, R. J., & Sheu, E. Y. (1996). Development of solid properties and thermochemistry of asphalt binders in the 25-65°C temperature range. Energy & Fuels, 10(3), 855–864. doi:10.1021/ef9502564.

[8] Nivitha, M. R., Prasad, E., & Krishnan, J. M. (2019). Transitions in unmodified and modified bitumen using FTIR spectroscopy. Materials and Structures/Materiaux et Constructions, 52(1), 1–11. doi:10.1617/s11527-018-1308-7.

[9] Williams, M. L., Landel, R. F., & Ferry, J. D. (1955). The Temperature Dependence of Relaxation Mechanisms in Amorphous Polymers and Other Glass-forming Liquids. Journal of the American Chemical Society, 77(14), 3701–3707. doi:10.1021/ja01619a008.

[10] Ferry, J. D. (1980). Viscoelastic properties of polymers. John Wiley & Sons, Hoboken, United States.

[11] Rajan, S., Sutton, M. A., Oseli, A., Emri, I., & Matta, F. (2017). Linear viscoelastic creep compliance and retardation spectra of bitumen impregnated fiberglass mat and polymer modified bitumen. Construction and Building Materials, 155, 664–679. doi:10.1016/j.conbuildmat.2017.08.030.

[12] Zoorob, S. E., Mturi, G. A., Sangiorgi, C., Dinis-Almeida, M., & Habib, N. Z. (2018). Fluxing as a new tool for bitumen rheological characterization and the use of time-concentration shift factor (AC). Construction and Building Materials, 158, 691–699. doi:10.1016/j.conbuildmat.2017.10.020.

[13] Lesueur, D. (2009). The colloidal structure of bitumen: Consequences on the rheology and on the mechanisms of bitumen modification. Advances in Colloid and Interface Science, 145(1–2), 42–82. doi:10.1016/j.cis.2008.08.011.

[14] Cheung, C. Y., &Cebon, D. (1997). Experimental study of pure bitumens in tension, compression, and shear. Journal of Rheology, 41(1), 45–74. doi:10.1122/1.550858.

[15] Atul Narayan, S. P., Murali Krishnan, J., Little, D. N., & Rajagopal, K. R. (2016). Mechanical behaviour of asphalt binders at high temperatures and specification for rutting. International Journal of Pavement Engineering, 18(10), 916–927. doi:10.1080/10298436.2015.1126272.

[16] Maze, M. (1996). Viscosity of EVA Polymer-Modified Bitumens: Modelling. No. 5170 Section 5. Euraspahlt&Eurobitume Congress, 7-10 May, 1996, Strasbourg, France.

[17] Salomon, D., & Zhai, H. (2002). Ranking asphalt binders by activation energy for flow. Journal of Applied Asphalt Binder Technology, 2(2), 52-60.

[18] Dongre, R., Myers, L., D'Angelo, J., Paugh, C., & Gudimettla, J. (2005). Field evaluation of Witczak and Hirsch models for predicting dynamic modulus of hot-mix asphalt (with discussion). Journal of the Association of Asphalt Paving Technologists, 74.

[19] Salomon, D., & Zhai, H. (2004). Asphalt binder flow activation energy and its significance for compaction effort. Proceedings of 3rdEuroasphalt&Eurobitume congress, 12-14 May 2004, Vienna, Austria.

[20] Saboo, N., Singh, B., & Kumar, P. (2019). Development of High-Temperature Ranking Parameter for Asphalt Binders Using Arrhenius Model. Journal of Materials in Civil Engineering, 31(12), 4019297. doi:10.1061/(asce)mt.1943-5533.0002965.

[21] Garća-Morales, M., Partal, P., Navarro, F. J., Marťnez-Boza, F., Gallegos, C., González, N., González, O., & Muñoz, M. E. (2004). Viscous properties and microstructure of recycled EVA modified bitumen. Fuel, 83(1), 31–38. doi:10.1016/S0016-2361(03)00217-5.

[22] Ait-Kadi, A., Brahimi, B., &Bousmina, M. (1996). Polymer blends for enhanced asphalt binders. Polymer Engineering & Science, 36(12), 1724–1733. doi:10.1002/pen.10568.

[23] Wang, H., Liu, X., Apostolidis, P., & Scarpas, T. (2018). Rheological behavior and its chemical interpretation of crumb rubber modified asphalt containing warm-mix additives. Transportation Research Record, 2672(28), 337–348. doi:10.1177/0361198118781376.

[24] Jamshidi, A., Hamzah, M. O., Shahadan, Z., & Yahaya, A. S. (2015). Evaluation of the Rheological Properties and Activation Energy of Virgin and Recovered Asphalt Binder Blends. Journal of Materials in Civil Engineering, 27(3), 4014135. doi:10.1061/(asce)mt.1943-5533.0001024.

[25] Luo, X., Gu, F., & Lytton, R. L. (2019). Kinetics-based aging prediction of asphalt mixtures using field deflection data. International Journal of Pavement Engineering, 20(3), 287–297. doi:10.1080/10298436.2017.1293262.

[26] Luo, X., Gu, F., & Lytton, R. L. (2015). Prediction of field aging gradient in asphalt pavements. Transportation Research Record, 2507(1), 19–28. doi:10.3141/2507-03.

[27] Haider, S. W., Mirza, M. W., Thottempudi, A. K., Bari, J., &Baladi, G. Y. (2011). Characterizing Temperature Susceptibility of Asphalt Binders Using Activation Energy for Flow. Transportation and Development Institute Congress 2011. doi:10.1061/41167(398)48.

[28] Notani, M. A., Arabzadeh, A., Satvati, S., TarighatiTabesh, M., GhafariHashjin, N., Estakhri, S., & Alizadeh, M. (2020). Investigating the high-temperature performance and activation energy of carbon black-modified asphalt binder. SN Applied Sciences, 2(2), 1–12. doi:10.1007/s42452-020-2102-z.

[29] Raouf, M. A., & Williams, R. C. (2010). Temperature and shear susceptibility of a nonpetroleum binder as a pavement material. Transportation Research Record, 2180(2180), 9–18. doi:10.3141/2180-02.

[30] Ingram, L., Mohan, D., Bricka, M., Steele, P., Strobel, D., Crocker, D., Mitchell, B., Mohammad, J., Cantrell, K., & Pittman, C. U. (2008). Pyrolysis of wood and bark in an auger reactor: Physical properties and chemical analysis of the produced bio-oils. Energy and Fuels, 22(1), 614–625. doi:10.1021/ef700335k.

[31] ASTM D2872-22. (2022). Standard Test Method for Effect of Heat and Air on a Moving Film of Asphalt (Rolling Thin-Film Oven Test). ASTM International, Pennsylvania, United States. doi:10.1520/D2872-22.

[32] ASTM D6521-22. (2022). Standard Practice for Accelerated Aging of Asphalt Binder Using a Pressurized Aging Vessel (PAV). ASTM International, Pennsylvania, United States. doi:10.1520/D6521-22.

[33] Kalelkar, C., Lele, A., & Kamble, S. (2010). Strain-rate frequency superposition in large-amplitude oscillatory shear. Physical Review E - Statistical, Nonlinear, and Soft Matter Physics, 81(3), 31401. doi:10.1103/PhysRevE.81.031401.

[34] ASTM D7405. (2015). Standard Test Method for Multiple Stress Creep and Recovery (MSCR) of Asphalt Binder Using a Dynamic Shear Rheometer. ASTM International, Pennsylvania, United States.